Impact of the COVID-19 pandemic related to lockdown measures on tropospheric NO2 columns over Île-de-France

Andrea Pazmino, Matthias Beekmann, Florence Goutail, Dmitry Ionov, Ariane Bazureau, Manuel Nunes-Pinharanda, Alain Hauchecorne, Sophie Godin-Beekmann

Atmos. Chem. Phys., 21, 18303–18317, 2021
https://doi.org/10.5194/acp-21-18303-2021

Atmospheric Chemistry and Physics
Open Access
EGU

Research article

Impact of the COVID-19 pandemic related to lockdown measures on tropospheric NO_2 columns over Île-de-France

Andrea Pazmiño[1], Matthias Beekmann[2], Florence Goutail[1], Dmitry Ionov[3], Ariane Bazureau[1], Manuel Nunes-Pinharanda[1], Alain Hauchecorne[1], and Sophie Godin-Beekmann[1]

[1]LATMOS/IPSL, UVSQ, Université Paris-Saclay, Sorbonne Université, CNRS, Guyancourt, France
[2]LISA/IPSL, UMR CNRS 7583, Université Paris Est Créteil, Université de Paris, Créteil, France
[3]Department of Atmospheric Physics, University of Saint Petersburg, Saint Petersburg, Russia

Correspondence: Andrea Pazmiño (andrea.pazmino@latmos.ipsl.fr)

Received: 2 June 2021 – Discussion started: 18 June 2021
Revised: 6 October 2021 – Accepted: 26 October 2021 – Published: 17 December 2021

Abstract. The evolution of NO_2, considered as a proxy for air pollution, was analyzed to evaluate the impact of the first lockdown (17 March–10 May 2020) over the Île-de-France region (Paris and surroundings). Tropospheric NO_2 columns measured by two UV-Visible Système d'Analyse par Observation Zénithale (SAOZ) spectrometers were analyzed to compare the evolution of NO_2 between urban and suburban sites during the lockdown. The urban site is the observation platform QualAir (48°50′ N / 2°21′ E) at the Sorbonne University Pierre and Marie Curie Campus in the center of Paris. The suburban site is located at Guyancourt (48°46′N / 2°03′E), Versailles Saint-Quentin-en-Yvelines University, 24 km southwest of Paris. Tropospheric NO_2 columns above Paris and Guyancourt have shown similar values during the whole lockdown period from March to May 2020. A decade of data sets were filtered to consider air masses at both sites with similar meteorological conditions. The median NO_2 columns and the surface measurements of Airparif (Air Quality Observatory in Île de France) during the lockdown period in 2020 were compared to the extrapolated values estimated from a linear trend analysis for the 2011–2019 period at each station. Negative NO_2 trends of -1.5 Pmolec. $cm^{-2}\,yr^{-1}$ ($\sim -6.3\,\%\,yr^{-1}$) are observed from the columns, and trends of $-2.2\,\mu g\,m^{-3}\,yr^{-1}$ ($\sim -3.6\,\%\,yr^{-1}$) are observed from the surface concentration.

The negative anomaly in tropospheric columns in 2020 attributed to the lockdown (and related emission reductions) was found to be 56 % at Paris and 46 % at Guyancourt, respectively. A similar anomaly was found in the data of surface concentrations, amounting to 53 % and 28 % at the urban and suburban sites, accordingly.

1 Introduction

Megacities can be considered as being a hotspot of anthropogenic pollution due to the concentration of population and human activities. People living in urban areas are exposed to air quality levels that are often poorer than the World Health Organization (WHO) recommended limits (WHO, 2006). In 2020, the emergence of a novel coronavirus that caused the COVID-19 pandemic in many countries around the world prompted the governments of the affected states to apply restrictive regulations. Most countries implemented lockdown measures (restrictions on people's movements) to limit the progression of the COVID-19 pandemic. As a result, urban areas have become interesting laboratories for analyzing the impact of these measures on air quality. Atmospheric concentrations of air pollutants in megacities were expected to decrease as a direct impact of the air and road traffic activity drop during the lockdown period. Observations of the TROPOspheric Monitoring Instrument (TROPOMI) instrument on board the Copernicus Sentinel 5-Precursor (S5P) satellite (Veefkind et al., 2012) were the earliest ones to be presented by the media to show the significant decrease in tropospheric NO_2 columns in the Hubei province in China (20 %–50 % in urban areas; Ding et al., 2020), which was the first region affected by COVID-19 in December 2019. Indeed, tropospheric NO_2 is considered as a good proxy for NO_x ($NO_x = NO + NO_2$) concentrations since NO is rapidly converted into NO_2 by the photochemical cycle involving tropospheric ozone. NO_x levels are directly linked to human activities; for example, over the Île-de-France region, in which the greater Paris region is imbedded, and for the year 2018, road traffic contributed to 53 % of NO_x emissions, followed by industry (13 %; including also energy and waste treatment), residential heating (11 %) and airports (9 %; https://www.airparif.asso.fr/surveiller-la-pollution/les-emissions, last access: August 2021).

Many studies have focused on NO_2 reductions due to lockdowns in 2020 at specific cities in China (Ding et al., 2020; Griffith et al., 2020) and in other affected countries (Bauwens et al., 2020; Prunet et al., 2020) using only satellite observations (Bauwens et al., 2020; Liu et al., 2020; Koukouli et al., 2021) or, additionally, ground-based instruments (Prunet et al., 2020; Biswal et al., 2021). Other studies analyzed the lockdown period using in situ monitoring networks in the cities (Baldasano, 2020; Krecl et al., 2020; Biswal et al., 2021). Model simulations were also analyzed to assess the respective NO_2 decreases (Liu et al., 2020; Menut et al., 2020; Koukouli et al., 2021).

The objective of this study is to quantify the effect of NO_2 decreases due to the lockdown by considering the long-term variability and meteorological conditions over the Île-de-France region during the last decade, using different data sets characterizing the lockdown impact at a local scale, with in situ instrumentation, and at a larger scale, including a large part of the agglomeration with tropospheric column measurements. In total, two complementary sites are used, with one in the center of Paris and the other one in the peripheral zone, to highlight the possibly heterogeneous impact of lockdown in the Île de France region. The originality of the study is to rely not only on a single reference year before the COVID-19 pandemic that could strongly bias the study but on a long, decadal data set, in order to account for NO_2 variability over a longer period. This allows, in addition, the calculation of long-term NO_2 column changes over the Paris region. Specific data filtering, using wind speed and direction, is applied in order to isolate the data which are affected by local pollution in the greater Paris area and to consider the changes in meteorological conditions for the different years.

This paper is organized as follows. Observations of tropospheric and surface amounts of NO_2 by ground-based and satellite measurements are presented in Sect. 2, as well as the wind data from European reanalysis. The description of the method used to discriminate specific data to calculate the NO_2 decrease in 2020, taking into account similar meteorological conditions, is presented in Sect. 3. The results of NO_2 decreases in 2020 due to the lockdown are shown in Sect. 4 for the different data sets. The results of NO_2 level reductions in respect to the literature findings are discussed in Sect. 5. Conclusions are finally presented in Sect. 6.

2 NO_2 data

Tropospheric NO_2 columns measured by two ground-based Système d'Analyse par Observation Zénithale (SAOZ) instruments were analyzed to trace and intercompare the evolution of NO_2 in the urban and suburban regions of Île-de-France. The analysis was supplemented by a study of NO_2 column satellite measurements using the TROPOMI instrument. In addition, the in situ measurements of NO_2 surface concentrations from the Airparif air quality network were also considered. In this work, the 10-year period of 2011–2020, with the first year corresponding to the start of the SAOZ measurements at the suburban site of Guyancourt, was considered. Table 1 shows the ground-based stations, type of instrument and geographical coordinates, and Fig. 1 shows the location of each station in the Île-de-France region.

2.1 Tropospheric columns

2.1.1 SAOZ data

The NO_2 tropospheric columns in the Île-de-France region are measured by two ground-based SAOZ instruments (Pommereau and Goutail, 1988) that are part of French research infrastructure of ACTRIS (Aerosols, Clouds and Trace gases Research Infrastructure). The first one was installed in 2005 at the observation platform of QualAir (http://qualair.aero.jussieu.fr/, last access: January 2021) at the Sorbonne University in Paris (urban station) and the second one has been operational at the LATMOS (Laboratoire Atmosphères, Observations Spatiales) laboratory in Guyancourt (southwestern suburban station) since 2011. SAOZ is a UV-Visible spectrometer primarily designed for monitoring the stratospheric ozone and NO_2 during twilight observations in the frame of the NDACC (Network for the Detection of Atmospheric Composition Change; see Hendrick et al., 2011, for a description of retrieval). The long-term data series of SAOZ instruments were compared with data from most satellite missions to validate or monitor their performance. For example, SAOZ instruments participated in the validation of the latest satellite mission (Sentinel-5 Precursor) launched on October 2017 for the measurements of ozone (Garane et al., 2019) and stratospheric NO_2 (Verhoelst et al., 2021) columns.

During the day, SAOZ observations are sensitive to increased tropospheric NO_2 amounts in polluted regions (Tack et al., 2015). Every ∼2 min, the sunlight backscattered by the atmosphere in the zenith direction of SAOZ is acquired, and the DOAS (differential optical absorption spectroscopy) method (Platt and Stutz, 2008) is applied in the NO_2 absorptions bands to obtain the respective slant column densities. The stratospheric NO_2 columns are removed from slant columns to retrieve the tropospheric NO_2 for solar zenith

Figure 1. Locations of the Airparif (red points) and SAOZ (blue points) stations. The black dashed line corresponds to the distance between both SAOZ stations. Map data © OpenStreetMap contributors 2021. Distributed under the Open Data Commons Open Database License (ODbL) v1.0.

Table 1. Ground-based stations used in this study, including the station, place, instrument and geographical coordinates.

Station	Place	Instrument	Lat, long
Paris	QualAir; Sorbonne-Université, Paris (fifth district)	SAOZ	48°50′ N, 2°21′ E
Guyancourt	LATMOS; Guyancourt	SAOZ	48°46′ N, 2°03′ E
CELES	Quai des Célestins; Paris (fifth district)	Airparif	48°51′ N, 2°21′ E
PA13	Parc de Choisy; park in Paris (13th district)	Airparif	48°49′ N, 2°21′ E
PA07	Allée des Refuzniks; Paris (seventh district)	Airparif	48°51′ N, 2°17′ E
EIFF3	300 m top of Eiffel Tower; Paris (seventh district)	Airparif	48°51′ N, 2°17′ E
VERS	Versailles	Airparif	48°48′ N, 2°08′ E

angles (SZAs) lower than 80° (see Dieudonné et al., 2013, for a detailed description of the SAOZ tropospheric NO_2 retrieval). The SAOZ data set of tropospheric NO_2 measurements at Paris was used in different studies to relate the NO_2 concentrations at the surface with the integrated NO_2 column in the boundary layer (Dieudonné et al., 2013) to interpret ozone measurements (Klein et al., 2017) and the seasonal cycle of the ozone gradient (Ancellet et al., 2020).

SAOZ tropospheric NO_2 columns are available at the SAOZ web page (http://saoz.obs.uvsq.fr/SAOZ_tropo_Paris.html, last access: 1 January 2021 and http://saoz.obs.uvsq.fr/SAOZ_tropo_Guyancourt.html, last access: 1 January 2021). These data were averaged daily between 06:00 and 18:00 UT and between 11:00 and 14:00 UT for comparison with satellite observations.

2.1.2 TROPOMI data

Tropospheric NO_2 columns retrieved by TROPOspheric Monitoring Instrument (TROPOMI) aboard Sentinel 5 Precursor (S5P) satellite (Veefkind et al., 2012) launched in October 2017 were also used to discriminate air masses above SAOZ instruments benefiting from the high spatial resolution of this instrument ($3.5 \times 7\,km^2$ and $3.5 \times 5.5\,km^2$ since August 2019). TROPOMI is a passive-sensing hyperspectral nadir-viewing imager, aboard a near-polar sun synchronous orbit satellite at an altitude of 817 km, with an overpass at 13:30 local time and practically daily global coverage.

Retrieval applied on TROPOMI data allows the distinction between tropospheric, stratospheric and total NO_2 columns. The algorithm was adapted from the DOMINO/TEMIS (Dutch OMI NO_2/Tropospheric Emission Monitoring Internet Service) approach for the ozone monitoring instrument (OMI; Boersma et al., 2007, 2011), based on the DOAS method to obtain slant column densities (SCDs) of NO_2 that are assimilated to the TM5-MP chemical transport model (CTM) to separate the SCD. The CTM runs using 0–12 h forecast meteorological data from the European Centre for Medium-Range Weather Forecasts (ECMWF) corresponding to the offline product. Finally, each slant column is converted to vertical column using the precalculated air mass factor (AMF) look-up tables. A detailed description can be found at the TROPOMI web page (http://www.tropomi.eu/data-products/nitrogen-dioxide, last access: January 2021).

Van Geffen et al. (2020) analyzed the uncertainties of the SCD of TROPOMI and compared them to OMI-QA4ECV data (Boersma et al., 2018). They show a very good agreement over a remote Pacific Ocean sector, with a correlation of 0.99, but values with 5 % higher than the OMI-QA4ECV ones. Verhoelst et al. (2021) compared NO_2 total, tropospheric and stratospheric columns with the data of ground-based instruments of Pandora, multi-axis differential optical absorption spectroscopy (MAX-DOAS) and zenith-scattered light DOAS (ZSL-DOAS or SAOZ) distributed around the world. Observations from MAX-DOAS were used for tropospheric comparisons since they are sensitive to absorbers in the lowest few kilometers of the atmosphere (Hönninger et al., 2004). A negative bias from 23 % to 37 % is observed in the cases of clean to slightly polluted conditions. In the case of highly polluted areas, the bias can reach 51 %.

TROPOMI tropospheric NO_2 columns have been widely used to estimate the reduction in NO_2 amounts linked to the lockdown in 2020, which was implemented in different countries to prevent the spread of COVID-19 (e.g., Bauwens et al., 2020; Ding et al., 2020; Liu et al., 2020; Biswal et al., 2021; Koukouli et al., 2021).

In their validation paper against consolidated ground-based data, Verhoelst et al. (2021) used TROPOMI's tropospheric columns of NO_2 with a quality assurance (QA) value higher than 0.75 to remove cloudy scenes presenting cloud radiance fraction higher than 0.5, snow- or ice-covered scenes and problems in the retrieval. In our study, we have decided to use a less restrictive threshold of 0.5 in order to enhance the number of days and to avoid biassing the results towards clear-day conditions. This resulted in doubling the number of data taken into account. The monthly mean NO_2 tropospheric columns of TROPOMI present a similar seasonal evolution within 2σ for both QA values (not shown).

TROPOMI tropospheric NO_2 columns are available at the Copernicus web page (https://s5phub.copernicus.eu, last access: March 2021).

2.2 Surface concentrations

Airparif is a network of standard in situ sensors to monitor air quality over the Île-de-France region. One of the key variables measured by Airparif is NO_2. Hourly NO_2 concentrations are measured at most of the stations. The concentrations are measured by chemiluminescence (Fontijn et al., 1970), where the NO_2 amount is obtained after a reduction to NO on a heated molybdenum converter. This kind of in situ sensor can overestimate ambient NO_2 concentrations due to interferences with the non-NO_x fraction of reactive nitrogen (NO_z). As an example, for urban sites in Mexico City, Dunlea et al. (2007) found an average NO_2 overestimation for this type of sensor by 22 %.

The Airparif network is formed by the (1) so-called traffic stations located at the edge of major traffic axes, (2) urban background stations located in the city but not in the immediate vicinity of emission sources, (3) suburban and rural stations, and, finally, a station installed at the top of the Eiffel Tower at an altitude of 300 m.

In this study, two Airparif sites near the SAOZ of Paris were used, with one being considered as a traffic site (Quai de Célestins) and the other as urban (Paris 13th). Airparif data of Versailles, the nearest station to the SAOZ of Guyancourt, were used to represent the suburban site. Finally, two more stations at the base (Paris 7) and at the top of the Eiffel Tower were considered to compare the evolution of the NO_2 concentration at different altitudes in the boundary layer. Data were obtained from Airparif web page (https://data-airparif-asso.opendata.arcgis.com/, last access: 22 January 2021). Daily average data between 06:00 and 18:00 UT are used in this study as for the SAOZ instrument.

2.3 ERA5 reanalysis

ERA5 is the latest reanalysis of the ECMWF (European Centre for Medium-Range Weather Forecasts) generated by Copernicus Climate Change Service. ERA5 is produced by the Integrated Forecast System (IFS) CY41r2 version, released in 2016, with a 10-member 4D-Var assimilation with windows of 12 h each. The horizontal grid resolution is $\sim$31 km with 137 hybrid vertical levels up to 0.01 hPa (Hersbach et al., 2020). In addition to the significant increase in the horizontal and vertical resolution of ERA5, as well as the 10-year experience of the model forecast and assimilation, new and reprocessed observational data records were considered. Further information can be found in online documents at the ECMWF web page (https://confluence.ecmwf.int/display/CKB/ERA5, last access: January 2021).

ERA5 surface winds over Europe have been validated with wind observations from 245 stations in Europe, including two stations in Île de France (Molina et al., 2021). The conclusion is that ERA5 is able to reproduce the wind speed from hourly to monthly time frequencies for any location in Europe with a Pearson's correlation coefficient varying from 0.6 to 0.85 on an hourly scale and 0.9 to 0.95 on a 24 h scale.

In this study, wind speed and direction at 950 hPa (mid-altitude of the convective boundary layer) were extracted from the 0.25° horizontal resolution in latitude and longitude data (over the 48.75° N, 49.00° N and 2.00° E, 2.50° E region) at noon. The available quality-checked final product was considered for 1 January 2011 to 31 October 2020 and a provisional product for November–December 2020, where the latter is not really expected to differ from the final product (Hersbach et al., 2020).

3 Methodology

The evaluation of the lockdown effects on atmospheric NO_2 amounts is performed by selecting air masses moving from the Parisian agglomeration to the suburban region. The objective is to consider only the days on which air masses for

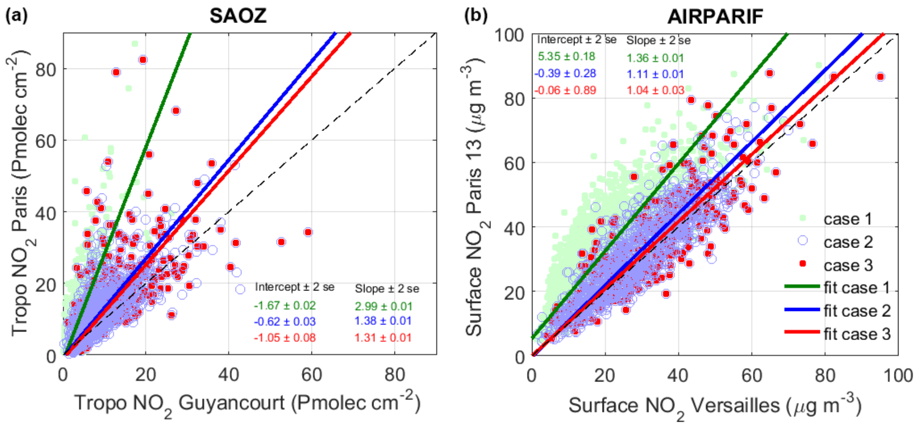

Figure 2. Scatterplots of tropospheric **(a)** and surface **(b)** NO_2 measurements at Paris as a function of measurements at the suburban station (Guyancourt and Versailles, respectively) for different levels of t (see Eq. 1). Linear fits of the different conditions are represented in green (case 1), blue (case 2) and red (case 3; see the text). The 1 : 1 line is represented by the black dashed line. The estimated slope and its standard error are also shown for each case.

both sampling sites have a long enough residence time over the Paris area and have been influenced by local pollution. In this work, the sampling filter of the air masses coming particularly from the Parisian agglomeration was determined with the purpose of evaluating the decrease in human activities linked to the lockdown in Paris at both sites. The downwind direction from Paris to Guyancourt is privileged to filter out air masses originating from the western sector, which are mainly of oceanic origin and have not yet encountered many European emissions. Combined wind speed and direction are considered in this study to identify such days. This procedure aims at selecting data sets with similar meteorological conditions for different years, thus reducing the impact of interannual weather variability. The evolution of NO_2 concentrations and tropospheric columns at Airparif and SAOZ stations (Table 1) are considered. The data of NO_2 concentration measurements by in situ instruments and NO_2 tropospheric column measurements by SAOZ were averaged daily between 06:00 and 18:00 UT. The measurement data are filtered using the wind speed and direction of ERA5 analysis at noon to select the weather conditions in which the Guyancourt site receives air masses that have passed the Paris agglomeration. Equation (1) represents the estimated residential time, t, of air masses coming from the center of Paris to Guyancourt.

$$t = \cos\left(\mathrm{abs}\left(\mathrm{dir}_g - \theta_{\mathrm{era5}}\right) \times \pi/180\right) \times D/(v_{\mathrm{era5}}), \qquad (1)$$

where v_{era5} and θ_{era5} correspond to the speed and direction of the wind at 12:00 UT and 950 hPa (altitude level in the middle of the convective boundary layer), dir_g is the direction between Guyancourt and Paris (290°), and D is the approximate diameter of agglomeration (9.5 km) if we consider it as a circle.

Using this parameter, t, three types of days were distinguished, and for each class a linear fit between urban versus suburban observations was calculated, as follows:

1. air masses of the Parisian agglomeration not influencing Guyancourt or Versailles ($t < 0$)
2. air masses of the Parisian agglomeration influencing Guyancourt or Versailles ($t > 0$)
3. air masses of the Parisian agglomeration in a condition of weak wind influencing Guyancourt or Versailles, which is a subclass of the precedent one ($t > 30$ min).

Figure 2 shows the scatterplot of SAOZ tropospheric NO_2 of Paris and Guyancourt (left panel) and Airparif in situ NO_2 of Paris's 13th district and Versailles (right panel) for the 2011–2020 period. Case 1 is represented by light green points, case 2 by blue circles and case 3 by red dots. A linear orthogonal fit was applied for the three cases to highlight the relationship between urban and suburban stations for the different conditions of wind speed and direction. For each case, higher NO_2 amounts are observed at Paris, and the air masses at the surface present lower linear regression slopes than tropospheric columns. Case 1 presents the largest slopes, i.e., 2.99 ± 0.01 (2σ standard error) for SAOZ measurements and 1.36 ± 0.01 for Airparif, highlighting the importance of wind direction. In this case when Guyancourt is upwind of Paris, air masses pass over Guyancourt without having touched the agglomeration. Those air masses arriving in the center of Paris have crossed part of the agglomeration and then show larger NO_2 columns. Cases 2 and 3 correspond to air masses generally crossing first the Parisian agglomeration and then southwestern suburban region. They show slopes closer to unity. In the case of SAOZ, the slopes of 1.38 ± 0.01 and 1.31 ± 0.01 were obtained for cases 2 and 3,

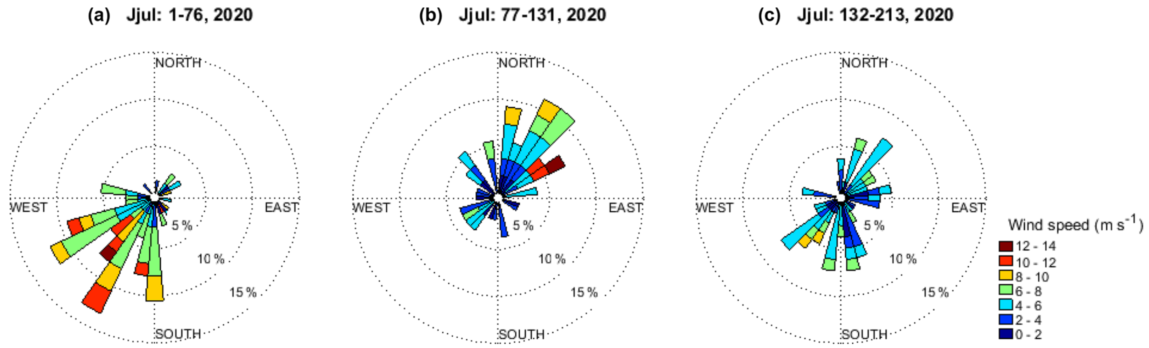

Figure 3. Panels **(a)** to **(c)** show the wind rose from 12:00 UT ERA5 data before (1 January–16 March), during (17 March–10 May) and after (11 May–31 July) the first lockdown in France in 2020. The color indicates the wind speed in meters per second ($m\,s^{-1}$). The frequency (in percent) is shown by the circles.

and the slopes of 1.11 ± 0.01 and 1.04 ± 0.03 in case of Airparif, respectively. For our study, the classification of days with air masses associated with $t > 30$ min will be considered because, in this case, air masses pass over both stations with weak wind, allowing for pollutant accumulation over the Paris agglomeration.

The poorer correlation observed with SAOZ data could be explained since different types of air masses could be sampled at Guyancourt in the tropospheric column, i.e., those passing through the agglomeration center and accumulating NO_2 when passing from the center to the edge (leading to larger columns at Guyancourt than at Paris) and those that have crossed only the limits of the agglomeration (leading to smaller columns at Guyancourt than at Paris).

4 Results

4.1 NO_2 evolution in 2020

The period preceding the lockdown represents meteorological conditions over Île-de-France mainly characterized by the high occurrence of oceanic air masses (see Fig. S3 of Petit et al., 2021) and fairly strong southwesterly winds (Fig. 3; left wind rose) preventing pollution events over this region. Changes in weather conditions 3 d after the implementation of the lockdown in 17 March 2020 (middle wind rose; Fig. 3) were mostly anticyclonic and contributed to the stagnation of pollutants in air masses advected from Paris to Guyancourt. Low wind speeds ($< 6\,m\,s^{-1}$) are predominantly northeasterly in the mid-March to mid-May period. The period after the end of the lockdown (Fig. 3; right wind rose) shows winds from southwesterly and northeasterly directions in the mid-May to July period.

Figure 4 shows the evolution of tropospheric NO_2 columns in Paris (red curve) and Guyancourt (blue curve) in 2020 as observed by SAOZ (top panel). Colored points correspond to the filtered data with $t > 0$ (open circles) and $t > 30$ min (solid points). The filtered air masses at Paris and Guyancourt present similar values for most of the cases with coincident daily events of increased tropospheric NO_2. Similar results are observed from in situ measurements at Airparif stations (Fig. 4; bottom panel). Vertical dashed lines are displayed in Fig. 4 to separate the four periods, i.e., before, during and after the lockdown and the last period of mixed restrictions (partial activities) after 31 October. The seasonal variability in NO_2 is well pronounced in the surface observations, with a minimum in June and a maximum in winter.

Table 2 shows different periods in 2020 related to restrictions imposed by French government to limit COVID-19 propagation. During period 1 (before the lockdown) only two particular events with high NO_2 values above both stations are detected at the same time ($t > 0$ min) by SAOZ instruments (19–25 January and 5–6 February). These events are also highlighted in the Airparif data. Only 1 d with $t > 30$ min is observed on 5 February. The frequent occurrence of oceanic air masses with high precipitation and wind speed leads to the advection of clean air masses above the Île-de-France region before the lockdown period (Viatte et al., 2021) and low NO_2 values are observed, which are lower than observed during period 2 (lockdown) for the suburban stations (Guyancourt and Versailles). A NO_2 peak is observed on 17 March, coincident to the start of the lockdown period, which could be linked to the massive departure of Parisian inhabitants. A change in weather conditions at the beginning of period 2, with low northeasterly wind speeds, promote the accumulation of polluted air masses over Île-de-France. Most of the days are characterized by a residential time of $t > 30$ min. Despite this situation, levels of tropospheric NO_2 remain low; this certainly illustrates the decrease in emissions during the lockdown period. Period 3 (after the lockdown) started on 11 May 2020, and NO_2 values remained low until the second week of July (the beginning of the school holidays), with NO_2 enhancement events comparable to period 2. Since then, higher NO_2 values of pollution events are observed by SAOZ and Airparif instruments, which show slight differences between the urban and suburban stations for days with $t > 30$ min. A less restrictive lock-

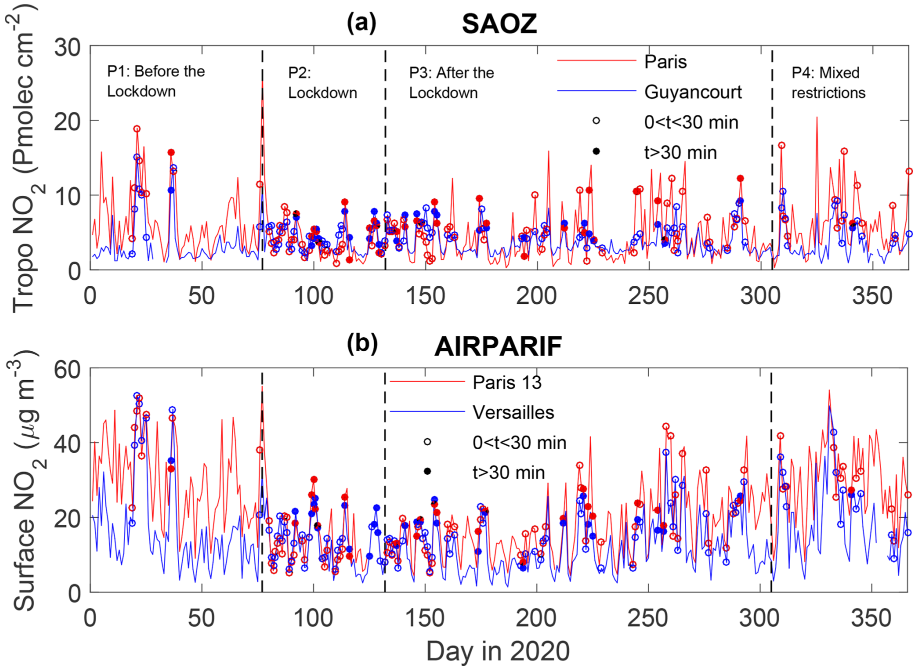

Figure 4. Evolution of tropospheric NO_2 columns **(a)** and surface NO_2 **(b)** in 2020 in Paris and the southwestern suburban stations. Vertical lines correspond to the day of the period change, i.e., 17 March, 11 May and 31 October.

down (open schools and less restrictive movement of people) was set up during period 4.

4.2 Comparison to previous years

4.2.1 Tropospheric NO_2 columns

TROPOMI tropospheric NO_2 measurements in 2020 were widely used to show a decrease in NO_2 amounts in different countries, which was attributed to policies restricting human activities by comparing the lockdown and pre-lockdown period or the same period in 2019 (e.g., Ding et al., 2020; Prunet et al., 2020; Siddiqui et al., 2020; Koukouli et al., 2021). SAOZ measurements between 11:00 and 14:00 UT were averaged to match overpass time of TROPOMI above the stations. TROPOMI data were previously filtered for the QA > 0.5 (see Sect. 2.1.2) and a radius of 5 km around SAOZ stations. Figure 5 shows the evolution of the monthly mean and two standard errors (2σ) of tropospheric NO_2 columns above Paris and Guyancourt stations since January 2019, as observed by SAOZ and TROPOMI (left panels). The standard error corresponds to the standard deviation of the mean divided by the root number of considered days. Similar intermonthly evolution is observed by both instruments, with a generally good agreement within $\pm 2\sigma$ and a correlation of 0.80 at Paris and 0.70 at Guyancourt. TROPOMI presents generally lower NO_2 values than SAOZ but within the 2σ uncertainty level. This is not the case in May 2020 (month 17 in Fig. 5) during which TROPOMI NO_2 amounts are significantly larger at the 2σ level than at SAOZ. Monthly mean values present a seasonal variation, reaching values above 10 Pmolec. cm^{-2} in winter in Paris, while they vary between 4 and 7 Pmolec. cm^{-2} in Guyancourt. The first months of 2020 present lower values compared to 2019, mostly due to weather conditions, while the March–May NO_2 decrease (month 15–17) is coincident with the lockdown period. A histogram of the differences between TROPOMI and SAOZ is also shown in Fig. 5 (right panels). A mean and median difference of -0.2 and $+0.12$ Pmolec. cm^{-2}, respectively, is obtained at the Paris station and of -0.6 and -0.7 Pmolec. cm^{-2}, respectively, at Guyancourt. It corresponds to a median relative difference of 2 % at the Paris station and -22 % at Guyancourt. The dispersion of the difference represented by the half of the 68 % interpercentile (IP68/2) is 2.9 and 1.6 Pmolec. cm^{-2}, respectively, at Paris and Guyancourt.

TROPOMI and SAOZ data selected for days with $t >$ 30 min were averaged between 11:00 and 14:00 UT for the period of the 2020 lockdown in France (17 March to 10 May), and median values were computed from the SAOZ and TROPOMI data for the 2011–2020 annual range (Fig. 6). TROPOMI NO_2 decrease in 2020 compared to 2019 is 35 ± 12 % for Paris and 22 ± 27 % for Guyancourt. Bauwens et al. (2020) found a decrease of 28 % during the first 21 d of lockdown over a 50 km region, centered over Paris, using TROPOMI and OMI data compared to same period in 2019. A larger tropospheric NO_2 decrease of about 47 % is found from SAOZ observations between 2019 and 2020 at both studied stations (see Fig. 6). Prunet et al. (2020) found

Table 2. The four periods in 2020 shown in Fig. 4 and the related restrictions imposed by the French government to limit the COVID-19 propagation.

	Periods in 2020	Restrictions
P1	1 Jan to 16 Mar	None
P2	17 Mar to 10 May	First lockdown, where nonessential stores, schools, cultural establishments, etc. are closed. Only travel <1 km and with a certificate are authorized. Home office/remote work is strongly suggested.
P3	11 May to 29 Oct	Gradual lifting of restrictions, where schools and nonessential stores are opened with physical distancing and masks. Travel is possible without a certificate. A curfew was imposed in mid-October. Home office/remote work is still recommended.
P4	31 Oct to 15 Dec	Second lockdown, where schools opened but universities still closed. Some activities are allowed, including some nonessential stores opened with strong restrictions. Some restrictions, such as travel of <1 km maximum, are relaxed at the end of November.

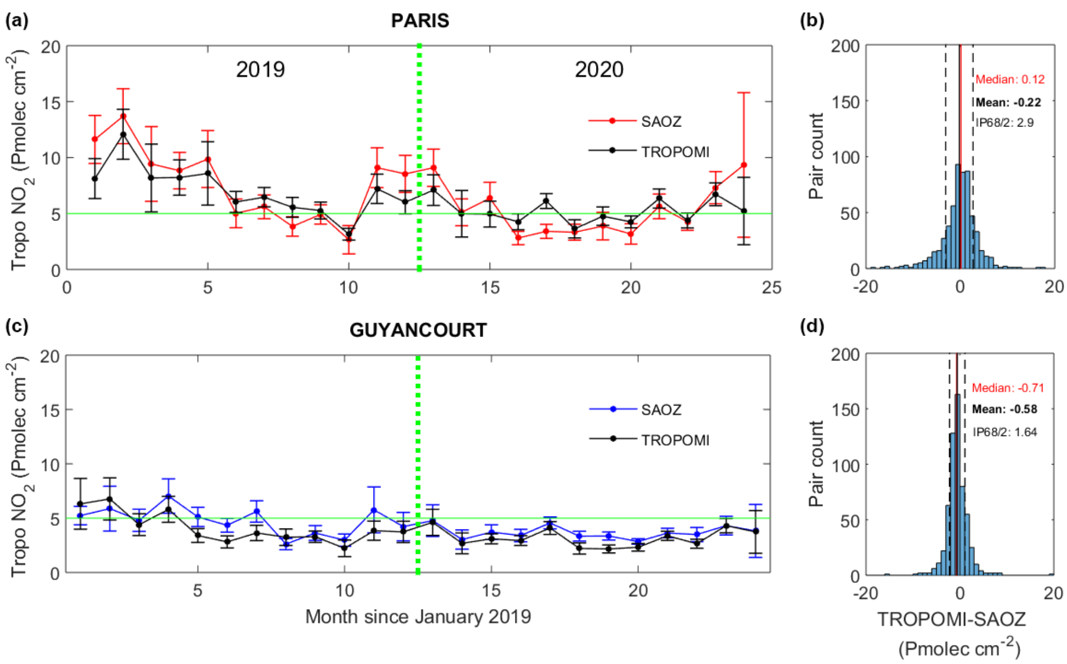

Figure 5. Monthly mean tropospheric NO_2 and 2σ standard error above Paris **(a)** and Guyancourt **(c)** measured by ground-based SAOZ instrument (colored lines) and TROPOMI satellite instrument (black lines). Histogram of TROPOMI-SAOZ differences at Paris **(b)** and Guyancourt **(d)**. Vertical lines represent the median, mean and dispersion by the half of the 68 % interpercentile range (IP68/2).

an even larger decrease in NO_2 values, varying from 52 % to 86 %, during the lockdown in a 120 km region around Paris using yearly 2019–2020 TROPOMI data and the city-scale NO_2 plume mass method.

It should be noted that the SAOZ data sets have shown a long-term negative trend since 2011. Font et al. (2019) have used in situ data to study the impact of policy initiatives in different megacities. They have shown a mean NO_2 decrease in roadside (background) sites of -2.9 (1.7) % yr^{-1} in Île-de-France for the 2010–2016 period, linked to the introduction of the Euro V regulations for heavy-duty vehicles in October 2009; other policies were implemented thereafter (e.g., Euro VI regulations in 2014). The trend of tropospheric NO_2 amounts needs to be considered to better quantify the effects of lockdown on air pollution, which cannot rely on the comparison with a single reference year as was done in many other studies (e.g., Bauwens et al., 2020; Prunet et al., 2020).

To better account for traffic-related pollution events in the daily averaged NO_2 columns, the full daytime data of tropospheric NO_2 measurements by SAOZ (SZA < 80°) of the

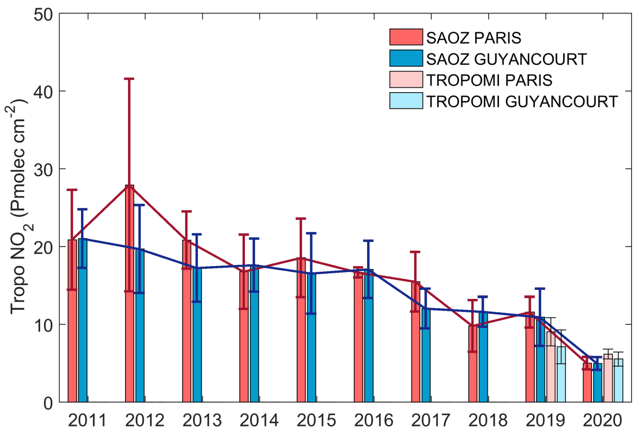

Figure 6. Tropospheric NO_2 median values of the 17 March–10 May period at Paris and Guyancourt from SAOZ observations (since 2011) and TROPOMI measurements (in 2019 and 2020). Error bars represent 1σ.

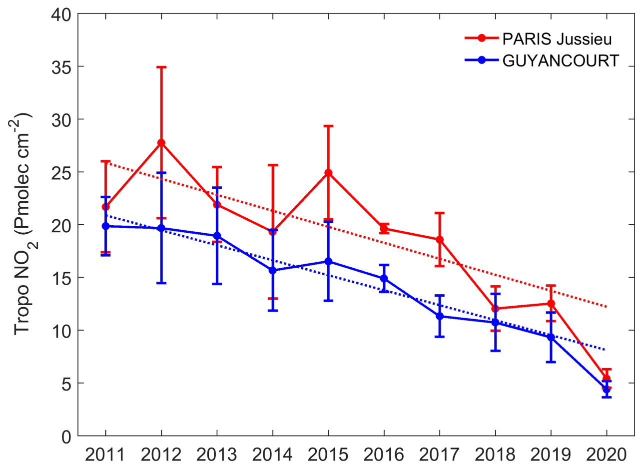

Figure 7. Interannual variability in the tropospheric NO_2 median values of the 17 March–10 May period at Paris and Guyancourt computed from SAOZ observations (since 2011). Error bars represent 1σ standard error. The computed robust fit is shown by the dotted color lines.

corresponding day were considered. The median value of the daily columns with $t > 30$ min was computed for each year during periods 2 and 3 above Paris and Guyancourt. Periods 1 and 4 were not considered since only 1 d with $t > 30$ min was observed above the stations during these periods in 2020. Period 3 was restricted to 11 May–15 July (period 3') to avoid the effect of NO_2 seasonal variations in the final median value. A robust regression fit (reweighted bisquare function to reduce weight of outliers far ~ 5 times from the median) was applied to period 2 and 3' to compute the trend for the 2011–2019 period. We will focus only on the period of lockdown since important NO_2 interannual variability in the period 3' does not present a 2σ significant slope value neither at Paris, nor at Guyancourt. Only the lockdown period presents a significant negative slope of $-1.51\pm0.48\,(1\sigma)$ Pmolec. $cm^{-2}\,yr^{-1}$ at Paris and $-1.42\pm0.14\,(1\sigma)$ Pmolec. $cm^{-2}\,yr^{-1}$ at Guyancourt, as shown in Fig. 7. These values correspond to a negative trend of $-5.86\pm1.92\,\%\,yr^{-1}$ at Paris and $-6.79\pm0.66\,\%\,yr^{-1}$ at Guyancourt relative to 2011. Previous studies have presented similar values over western Europe. Zhou et al. (2012) found significant negative trends in the 2004–2009 period, varying from $-4\,\%\,yr^{-1}$ to $-8\,\%\,yr^{-1}$, using OMI tropospheric NO_2 columns. Curier et al. (2014) computed the trend from the synergistic use of OMI NO_2 tropospheric columns and the chemistry transport model LOTOS-EUROS, finding significant negative trends of $5\,\%\,yr^{-1}$–$6\,\%\,yr^{-1}$. The year 2020 presents the lowest values of NO_2 at both stations (5.4 Pmolec. cm^{-2} at Paris and 4.4 Pmolec. cm^{-2} at Guyancourt) that are significantly different, at 1σ, from previous years (Fig. 7). The median value in 2020 is lower than the extrapolated value, using the computed 2011–2019 trend, by $55.6\pm15.7\,\%$ at Paris and $45.6\pm11.8\,\%$ at Guyancourt. If the tropospheric median column of NO_2 in 2019 had been used as a reference for comparison, slightly higher declines would have been obtained within $\pm1\sigma$:$56.7\pm9.1\,\%$ and $52.6\pm14.5\,\%$ at Paris and Guyancourt, respectively. Choosing other reference years would obviously yield different results, e.g., a slightly lower value at Paris ($55\pm10.7\,\%$) and an even higher value at Guyancourt ($58.9\pm12.5\,\%$) when using the year 2018 as a reference (Fig. 7). Moreover, choosing earlier years as a reference would pose the problem of NO_2 variability factors associated with both the lockdown and the long-term NO_2 reductions. This confirms the advantage of our method that calculates the reference from a decadal database and corrects for the long-term trend. It should be noted that the data filtering procedure based on meteorological conditions (wind speed and direction) significantly changes the result of the NO_2 reduction estimate in Guyancourt, making it statistically insignificant ($9.7\pm41.6\,\%$) if filtering is not applied; at the same time, the estimate for Paris has not changed much ($58.3\pm20.9\,\%$). Table 3 presents a summary of the NO_2 reductions in 2020, using different data sets described previously in the text. This indicates that the results at the Paris site located in the center of the agglomeration are not dependent, in 2020, on meteorological conditions. On the contrary, for the Guyancourt site at the edge of the agglomeration, selecting the days when the site is impacted by emissions within the agglomeration is crucial.

4.2.2 Surface NO_2 concentrations

The annual median NO_2 concentration at Airparif stations, since 2011 (Table 1), were computed from daily available hourly data during the lockdown period, filtered for the wind speed and direction as it has been done for the tropospheric NO_2 column ($t > 30$ min). Figure 8 presents the interannual variability in the NO_2 concentration at the five Airparif sta-

Table 3. Data set used to compute the NO_2 reductions in 2020, with the instrument, time period in universal time (UT) to calculate the daily mean value, the reference value and the application of the filter of the residential time. The last columns correspond to the corresponding computed reductions in percent for Paris and Guyancourt. Significant values at 1σ are in bold.

Data set	Daily mean (UT)	Reference	Filter	Paris	Guyancourt
TROPOMI	11:00–14:00	2019	Yes	**35**	22
SAOZ	11:00–14:00	2019	Yes	**47**	**47**
SAOZ	06:00-18:00	2019	Yes	**56.7**	**52.8**
SAOZ	06:00–18:00	2018	Yes	**55.0**	**58.9**
SAOZ	06:00–18:00	Trend in 2020	Yes	**55.6**	**45.6**
SAOZ	06:00–18:00	Trend in 2020	No	**59.3**	9.7

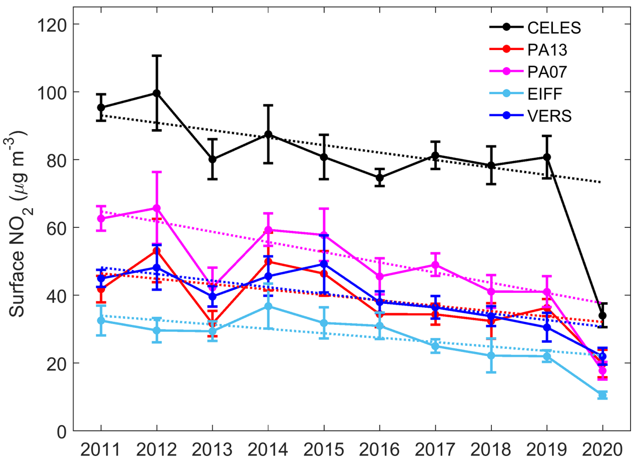

Figure 8. Similar to Fig. 7 but with the surface NO_2 concentration for different in situ sensors of Airparif network (see Table 1).

tions. In addition, the calculated robust fit for the decadal evolution at each station is shown. The background or urban stations (Paris 7 and 13) present similar interannual variability, with higher values at Paris's seventh district. The station of Quai de Célestins, in close proximity to local traffic, shows much higher values which are significantly different from those at other urban sites. The suburban station of Versailles presents similar values to Paris's 13th district at $\pm 1\sigma$. The observation station located at the Eiffel Tower at 300 m height near Paris's seventh district station shows the lowest values.

The five Airparif stations present negative trends from -3 to $-1.3\,\mu g\,m^{-3}\,yr^{-1}$, equivalent to $-4.6\,\%\,yr^{-1}$ to $2.4\,\%\,yr^{-1}$ (Table 4). Font et al. (2019) found a similar negative trend, varying from $-3.4\,\%\,yr^{-1}$ to $-2.4\,\%\,yr^{-1}$, for roadside stations in Paris for the 2010–2016 period. These trends appear to be less negative than those obtained from column measurements. Possible reasons for this are an increase in the NO_2 to NO_x emission ratio and a limitation of the available amount of O_3 for the NO to NO_2 conversion. Both factors affect the surface concentration than the boundary layer column more strongly, which could lead then to the different trend estimates.

Incomplete NO to NO_2 conversion is, for example, suggested by NO_2 and ozone concentrations of the same order of magnitude at Paris's urban background sites (Fig. 38 in Airparif, 2020). In such a situation, the NO_2 trends are both impacted by the NO_x emission and ozone trends. Figure 38 in Airparif (2020) cited above shows a strongly increasing ozone average urban background over Paris, e.g., 35 to 43 $\mu g\,m^{-3}$, respectively, for the 2007–2009 and 2017–2019 periods. This positive ozone trend buffers, to some extent, the negative NO_x emission trend.

However, while this reasoning would qualitatively explain the differences in trends between column and in situ measurements, it fails to explain differences in trends between different in situ sites in the sense that larger NO_x values would lead to smaller negative trends. This is not observed; on the contrary, the NO_2 trend is more negative at base of the Eiffel Tower than at altitude when NO_x becomes lower. Thus, the exact explanation of the differences in trends at different sites and heights still needs more investigation. In 2020, significant decreases, compared to the extrapolated value using the above-calculated linear trends, are observed at all stations and reach similar median values, which are slightly higher for the traffic station and slightly lower for Eiffel Tower observation station. The relative values of NO_2 reductions are shown in Table 4. Comparable values at 1σ are observed for traffic and urban stations in Paris, with lower values at Paris's 13th district, where the standard error is higher. Nevertheless, the reduction in NO_2 concentrations observed in absolute values is more important at traffic stations (such as CELES – Quai de Célestins) compared to the urban station (such as Paris's seventh district). The observation station installed at the Eiffel Tower at 300 m height presents a 53 % reduction that is identical to the station at Paris's seventh district, which is located at the base of the tower. The suburban station of Versailles presents the lowest reduction of 28.5 %, which is significantly different to other stations at 1σ, except for Paris's 13th district. It should be noted that both stations show an almost twice as large standard deviation of 14 %. The reasons for these lower values are not clear. It can be speculated that, at this suburban site, the relative contribution of residential heating to

Table 4. Airparif stations, type, the NO_2 trend $\pm 1\sigma$ in micrograms per cubic meter per year ($\mu g\,m^{-3}\,yr^{-1}$) and the NO_2 reduction in 2020, compared to the estimated value as a function of the computed trend.

Station	Type	Trend (2011–2019) $\pm 1\sigma$ ($\mu g\,m^{-3}\,yr^{-1}$) / (% yr^{-1})	Reduction in 2020 $\pm 1\sigma$ (%)
CELES	Traffic	-2.19 ± 0.85 / 2.36 ± 0.92	53.6 ± 5.4
PA13	Urban	-1.59 ± 1.04 / -3.34 ± 2.25	38.3 ± 14.6
PA07	Urban	-3.01 ± 0.81 / -4.65 ± 1.25	52.9 ± 8.4
EIFF	Observation	-1.30 ± 0.51 / -3.83 ± 1.49	52.8 ± 9.4
VERS	Suburban	-1.94 ± 0.58 / -4.02 ± 1.18	28.5 ± 13.1

NO_x sources is stronger than at Paris sites, and probably, these sources increased during the lockdown period due to the presence of people in their homes (Menut et al., 2020).

Collivignarelli et al. (2021) compared the NO_2 concentration observed by the traffic and urban stations of Airparif during the lockdown in 2020 to the same period in previous years (2017–2019). They found a decrease of 15 % for the urban stations and 33 % for traffic stations. However, when considering similar meteorological conditions with respect to rainfall, temperature and wind speed, the authors found a reduction of 51.5 % corresponding to traffic stations and approximately 45 % for background ones, similar to values obtained in this study.

5 Discussion

Various studies have been conducted to assess the impact of recent lockdowns on air quality in many countries around the world due to COVID-19 pandemic. In a number of works, the observed NO_2 contents were compared with the respective levels for the same period of previous years using ground-based and/or satellite measurements. Shi and Brasseur (2020) found a decrease in NO_2 concentrations in China by 50 %, compared to 2019 during the same period of the lockdown, and by 60 % ,compared to 2018, highlighting the interannual variability of NO_2 reductions that could depend on meteorological conditions or long-term variability. Other authors compared NO_2 amounts before and during the lockdown. For example, Siddiqui et al. (2020) observed a 46 % reduction in NO_2 tropospheric columns in India using satellite data, Liu et al. (2020) estimated a 48 % reduction in China before and during the Lunar New Year, which is 21 % more than in previous years 2015–2019 (given that a NO_2 reduction has been observed over the past years even without COVID), and Bauwens et al. (2020) deduced a 20 %–38 % reduction in western Europe. Many studies have considered specific techniques to limit the effect of meteorological conditions in their data. In the case of Paris, a 45 %–52 % reduction in NO_2 concentration was estimated by Collivignarelli et al. (2021), using equivalent temperature and wind speed days, and ~ 50 % was estimated by Barré et al. (2021), using a gradient boosting machine learning (GBML) technique. In the case of tropospheric NO_2 columns measured by satellite instruments, Prunet et al. (2020) estimated a 2-week-averaged reduction of NO_2 varying between 52 % and 86 %, using the city-scale NO_2 plume mass method for 16 March–26 April. In the present study, the long-term evolution was considered from 1 decade of measurements combined with air masses filtering based on slow wind speed and long residence time. The calculated reductions in the tropospheric NO_2 column and surface concentration are comparable in magnitude to the results of previous studies in western Europe, i.e., 46 %–56 % and 28 %–54 %, respectively.

Menut et al. (2020) compared the results of two special model calculations performed for the March 2020 lockdown period in western Europe. They used the Weather Research and Forecasting (WRF)-CHIMERE model for the following two simulations: one using a business-as-usual (BAU) scenario with classical emissions and the other one using a realistic scenario taking into account an estimate of the effect of lockdown measures on NO_2 in 2020. The authors found a maximum reduction of 43 % in the average NO_2 concentration over France. This simulation was based on a reduction in emissions of about 80 % in the transport sector and 40 % reduction in the industrial sector, but there was an increase in residential emissions during the second half of March, reducing emissions of NO_x probably by more than 50 % (taking into account the distribution of NO_x emissions as given by Citepa (https://www.citepa.org/fr/2020-nox/, last access: April 2021). Thus, NO_2 concentration reductions are slightly lower than NO_x emissions changes in these simulations, probably due to an increase in the NO_2/NO ratio for lower NO_x concentrations. This suggests that, at least when spatially averaged, NO_x emission reductions due to the lockdown are similar to those of NO_2 surface concentrations.

6 Conclusions

To assess the impact of France's policy decision to limit the spread of the SARS-CoV-2 virus by establishing a restrictive lockdown between 17 March and 10 May 2020, NO_2 surface concentrations and tropospheric columns over Île-de-France were analyzed, more specifically in Paris and suburban areas in the southwest of the agglomeration. Possible factors that can influence NO_2 changes, other than NO_x emissions reduction due to the lockdown, were considered. The data sets were partitioned to select the conditions of light winds moving air masses from Paris to a suburban area in the southwest. In addition, the known long-term reduction in NO_2 is also considered using the measurements in the previous decade. The tropospheric NO_2 reduction obtained from the SAOZ data is about 50 % (56 % at the Paris site and 46 % at the southwestern suburban site). These values are close to the literature data found for Europe within the estimated error bars (Barré et al., 2021; Prunet et al., 2020). This work highlights the ability of satellite TROPOMI measurements to distinguish between the tropospheric columns of urban and suburban sites, showing higher mean values at an urban station compared to a suburban one. The latter is also confirmed by the ground-based SAOZ measurement data. The agreement between the evolution of NO_2 in the troposphere observed at urban and suburban sites improves when selecting similar meteorological conditions. Surface NO_2 concentrations inside Paris are highly influenced by local pollution, and differences between the data of traffic and background urban sites are observed as expected. Surface concentrations were reduced by ~ 50 % at all stations (similar to $\pm 1\sigma$), except for the site in Paris's 13th district at Choisy Park that shows a lower reduction. The suburban station of Versailles presents NO_2 concentrations similar to Paris's 13th district, and the reduction in 2020 was 10 % lower, within the error bars.

The reductions at Paris sites during the lockdown are important, whether or not a filter was used to remove the effect of different meteorological conditions. On the contrary, selecting data according to air mass residence time over the agglomeration strongly changes the estimates of NO_2 reductions at the suburban sites. As expected, if filtering is not applied, lower NO_2 reductions are found for suburban sites, since the data sets include also measurements that are less affected by the agglomeration and closer to background conditions. If the long-term evolution is not considered, the computed reductions highly depend on the year of reference. In this study, a negative tropospheric NO_2 trend of -1.5 Pmolec. $cm^{-2}\,yr^{-1}$ (equivalent to ~ 6.3 % yr^{-1}) is observed. Surface NO_2 concentrations also show negative trends, with a mean value of $-2.2\,\mu g\,m^{-3}\,yr^{-1}$ (~ 3.6 % yr^{-1}).

In conclusion, the negative trend estimated during the last decade indicates the long-term benefits of the environmental measures taken to reduce NO_x emissions. The magnitude of the NO_2 supplementary reduction in 2020, which we calculate to be around 50 %, is consistent with the reduction in emissions associated with the lockdown in France, as suggested in a recent modeling study (Menut, 2020).

Data availability. The data used in this study are publicly available. Tropospheric NO_2 data can be accessed from SAOZ instruments at http://saoz.obs.uvsq.fr (SAOZ, 2021) and from the TROPOMI satellite instrument at https://s5phub.copernicus.eu (European Space Agency, 2021). Data under the ODbL license and NO_2 concentration data are available at https://data-airparif-asso.opendata.arcgis.com/ (Airparif, 2021). Wind speed and direction data from ERA5 can be found at https://confluence.ecmwf.int/display/CKB/ERA5 (ECMWF, 2021). The data of Airparif can be obtained directly by searching for the year (yyyy) and station name in the first column of Table 1 (https://data-airparif-asso.opendata.arcgis.com/datasets/YYYY-station/explore). An example for Quai des Célestins or CELES (Table 1) and the year 2020 is available at https://data-airparif-asso.opendata.arcgis.com/datasets/2020-celes/explore.

Author contributions. AP, FG and MP contributed to the processing, analysis and availability of the SAOZ data. AB and DI processed the TROPOMI data. AH provided ERA5 data for the area above Paris. MB developed the filter method to account for meteorological conditions. AP and SGB performed the statistical analysis. AP wrote the paper, with the assistance from all authors.

Competing interests. The contact author has declared that neither they nor their co-authors have any competing interests.

Disclaimer. Publisher's note: Copernicus Publications remains neutral with regard to jurisdictional claims in published maps and institutional affiliations.

Special issue statement. This article is part of the special issue "Quantifying the impacts of stay-at-home policies on atmospheric composition and properties of aerosol and clouds over the European regions using ACTRIS related observations (ACP/AMT inter-journal SI)". It is not associated with a conference.

Acknowledgements. The authors warmly thank the Institut National des Sciences de l'Univers (INSU) of the Centre National de la Recherche Scientifique (CNRS) and the Centre National d'Études Spatiales (CNES) for supporting the observations of the SAOZ instruments of the French research infrastructure of ACTRIS. The SAOZ instrument of Paris is hosted at the QualAir platform in the Sorbonne University and the Guyancourt instrument is at the SAOZ Unit/ACTRIS platform in Versailles Saint-Quentin-en-Yvelines University. We thank the Copernicus Services Data Hub for providing the TROPOMI/S5P data, Airparif for the in situ observations and ECMWF for ERA5 wind data. The authors thank the two anonymous referees for their constructive reviews.

Financial support. This research has been supported by the Centre National d'Etudes Spatiales (grant no. ValS5PSAOZ).

Review statement. This paper was edited by Eduardo Landulfo and reviewed by two anonymous referees.

References

Airparif: Open data, available at: https://data-airparif-asso.opendata.arcgis.com/, last access: 22 January 2021.

Airparif: Surveillance et information sur la qualité de l'air en Île-de-France – Bilan de l'année 2019, available at: https://www.airparif.asso.fr/sites/default/files/documents/2020-06/bilan-2019_0.pdf, (last access: August 2021), 2020.

Ancellet, G., Ravetta, F., Pelon, J., Pazmino, A., Klein, A., Dieudonné, E., Augustin, P., and Delbarre, H.: Ozone Lidar Observations in the City of Paris: Seasonal Variability and Role of The Nocturnal Low Level Jet, EPJ Web Conf., 237, 03022, https://doi.org/10.1051/epjconf/202023703022, 2020.

Baldasano, J.: COVID-19 lockdown effects on air quality by NO_2 in the cities of Barcelona and Madrid (Spain), Sci. Total Environ., 741, 140353, https://doi.org/10.1016/j.scitotenv.2020.140353, 2020.

Barré, J., Petetin, H., Colette, A., Guevara, M., Peuch, V.-H., Rouil, L., Engelen, R., Inness, A., Flemming, J., Pérez García-Pando, C., Bowdalo, D., Meleux, F., Geels, C., Christensen, J. H., Gauss, M., Benedictow, A., Tsyro, S., Friese, E., Struzewska, J., Kaminski, J. W., Douros, J., Timmermans, R., Robertson, L., Adani, M., Jorba, O., Joly, M., and Kouznetsov, R.: Estimating lockdown-induced European NO2 changes using satellite and surface observations and air quality models, Atmos. Chem. Phys., 21, 7373–7394, https://doi.org/10.5194/acp-21-7373-2021, 2021.

Bauwens, M., Compernolle, S., Stavrakou, T., Müller, J.-F., van Gent, J., Eskes, H., Levelt, P. F., van der A, R., Veefkind, J. P., Vlietinck, J., Yu, H, and Zehner, C.: Impact of coronavirus outbreak on NO_2 pollution assessed using TROPOMI and OMI observations, Geophys. Res. Lett., 47, e2020GL087978, https://doi.org/10.1029/2020GL087978, 2020.

Biswal, A., Singh, V., Singh, S., Kesarkar, A. P., Ravindra, K., Sokhi, R. S., Chipperfield, M. P., Dhomse, S. S., Pope, R. J., Singh, T., and Mor, S.: COVID-19 lockdown-induced changes in NO_2 levels across India observed by multi-satellite and surface observations, Atmos. Chem. Phys., 21, 5235–5251, https://doi.org/10.5194/acp-21-5235-2021, 2021.

Boersma, K. F., Eskes, H. J., Veefkind, J. P., Brinksma, E. J., van der A, R. J., Sneep, M., van den Oord, G. H. J., Levelt, P. F., Stammes, P., Gleason, J. F., and Bucsela, E. J.: Near-real time retrieval of tropospheric NO_2 from OMI, Atmos. Chem. Phys., 7, 2103–2118, https://doi.org/10.5194/acp-7-2103-2007, 2007.

Boersma, K. F., Eskes, H. J., Dirksen, R. J., van der A, R. J., Veefkind, J. P., Stammes, P., Huijnen, V., Kleipool, Q. L., Sneep, M., Claas, J., Leitão, J., Richter, A., Zhou, Y., and Brunner, D.: An improved tropospheric NO_2 column retrieval algorithm for the Ozone Monitoring Instrument, Atmos. Meas. Tech., 4, 1905–1928, https://doi.org/10.5194/amt-4-1905-2011, 2011.

Boersma, K. F., Eskes, H. J., Richter, A., De Smedt, I., Lorente, A., Beirle, S., van Geffen, J. H. G. M., Zara, M., Peters, E., Van Roozendael, M., Wagner, T., Maasakkers, J. D., van der A, R. J., Nightingale, J., De Rudder, A., Irie, H., Pinardi, G., Lambert, J.-C., and Compernolle, S. C.: Improving algorithms and uncertainty estimates for satellite NO_2 retrievals: results from the quality assurance for the essential climate variables (QA4ECV) project, Atmos. Meas. Tech., 11, 6651–6678, https://doi.org/10.5194/amt-11-6651-2018, 2018.

Collivignarelli, M. C., De Rose, C., Abbà, A, Baldi, M., Bertanza, G., Pedrazzani, R., Sorline, S., and Carnevale Miino, M.: Analysis of lockdown for CoViD-19 impact on NO_2 in London, Milan and Paris: What lesson can be learnt?, Process Saf. Environ., 146, 952–960, https://doi.org/10.1016/j.psep.2020.12.029, 2021.

Curier, R. L., Kranenburg, R., Segers, A. J. S., Timmermans, R. M. A., and Schaap, M.: Synergistic use of OMI NO_2 tropospheric columns and LOTOS–EUROS to evaluate the NO_x emission trends across Europe, Remote Sens. Environ., 149, 58–69, https://doi.org/10.1016/j.rse.2014.03.032, 2014.

Dieudonné, E., Ravetta, F., Pelon, J., Goutail, F., and Pommereau, J.-P.: Linking NO_2 surface concentration and integrated content in the urban developed atmospheric boundary layer, Geophys. Res. Lett., 40, 1247–1251, https://doi.org/10.1002/grl.50242, 2013.

Ding, J., van der A, R. J., Eskes, H. J., Mijling, B., Stavrakou, T., van Geffen, J. H. G. M., and Veefkind, J. P.: NO_x emissions reduction and rebound in China due to the COVID-19 crisis, Geophys. Res. Lett., 46, e2020GL089912, https://doi.org/10.1029/2020GL089912, 2020.

Dunlea, E. J., Herndon, S. C., Nelson, D. D., Volkamer, R. M., San Martini, F., Sheehy, P. M., Zahniser, M. S., Shorter, J. H., Wormhoudt, J. C., Lamb, B. K., Allwine, E. J., Gaffney, J. S., Marley, N. A., Grutter, M., Marquez, C., Blanco, S., Cardenas, B., Retama, A., Ramos Villegas, C. R., Kolb, C. E., Molina, L. T., and Molina, M. J.: Evaluation of nitrogen dioxide chemiluminescence monitors in a polluted urban environment, Atmos. Chem. Phys., 7, 2691–2704, https://doi.org/10.5194/acp-7-2691-2007, 2007.

European Centre for Medium-Range Weather Forecasts (ECMWF): ERA5: data documentation – CDS dataset documentation, ECMWF [data set], available at: https://confluence.ecmwf.int/display/CKB/ERA5, last access: 20 January 2021.

European Space Agency: Sentinel-5P Pre-Operations Data Hub, esa [data set], available at: https://s5phub.copernicus.eu, last access: 3 January 2021.

Font, A., Guiseppin, L., Blangiardo, M., Ghersi, V., and Fuller, G. W.: A tale of two cities: is air pollution improving in Paris and London?, Environ. Pollut., 249, 1–12, https://doi.org/10.1016/j.envpol.2019.01.040, 2019.

Fontijn, A., Sabadell, A. J., and Ronco, R. J.: Homogeneous chemiluminescent measurement of nitric oxide with ozone. Implications for continuous selective monitoring of gaseous air pollutants, Anal. Chem., 42, 575–579, https://doi.org/10.1021/ac60288a034, 1970.

Garane, K., Koukouli, M.-E., Verhoelst, T., Lerot, C., Heue, K.-P., Fioletov, V., Balis, D., Bais, A., Bazureau, A., Dehn, A., Goutail, F., Granville, J., Griffin, D., Hubert, D., Keppens, A., Lambert, J.-C., Loyola, D., McLinden, C., Pazmino, A., Pommereau, J.-P., Redondas, A., Romahn, F., Valks, P., Van Roozendael, M., Xu, J., Zehner, C., Zerefos, C., and Zimmer, W.: TROPOMI/S5P total ozone column data: global ground-based validation and consistency with other satellite missions, Atmos. Meas. Tech., 12, 5263–5287, https://doi.org/10.5194/amt-12-5263-2019, 2019.

Griffith, S., Huang, W.-S., Lin, C.-C., Chen, Y.-C., Chang, K.-E., Lin, T.-H., Wang, S.-Hg., and Lin, N.-H.: Long-range air pollution transport in East Asia during the first week of the COVID-19 lockdown in China, Sci. Total Environ., 741, 140214, https://doi.org/10.1016/j.scitotenv.2020.140214, 2020.

Hendrick, F., Pommereau, J.-P., Goutail, F., Evans, R. D., Ionov, D., Pazmino, A., Kyrö, E., Held, G., Eriksen, P., Dorokhov, V., Gil, M., and Van Roozendael, M.: NDACC/SAOZ UV-visible total ozone measurements: improved retrieval and comparison with correlative ground-based and satellite observations, Atmos. Chem. Phys., 11, 5975–5995, https://doi.org/10.5194/acp-11-5975-2011, 2011.

Hersbach, H., Bell, B., Berrisford, P., Hirahara, S., Horányi, A., Muñoz-Sabater, J., Nicolas, J., Peubey, C., Radu, R., Schepers, D., Simmons, A., Soci, C., Abdalla, S., Abellan, X., Balsamo, G., Bechtold, P., Biavati, G., Bidlot, J., Bonavita, M., Chiara, G., Dahlgren, P., Dee, D., Diamantakis, M., Dragani, R., Flemming, J., Forbes, R., Fuentes, M., Geer, A., Haimberger, L., Healy, S., Hogan, R. J., Hólm, E., Janisková, M., Keeley, S., Laloyaux, P., Lopez, P., Lupu, C., Radnoti, G., Rosnay, P., Rozum, I., Vamborg, F., Villaume, S., and Thépaut, J.-N.: The ERA5 Global Reanalysis, Q. J. Roy. Meteor. Soc., 146, 1999–2049, https://doi.org/10.1002/qj.3803, 2020.

Hönninger, G., von Friedeburg, C., and Platt, U.: Multi axis differential optical absorption spectroscopy (MAX-DOAS), Atmos. Chem. Phys., 4, 231–254, https://doi.org/10.5194/acp-4-231-2004, 2004.

Klein, A., Ancellet, G., Ravette, F., Thoas, J. L., and A. Pazmino: Characterizing the seasonal cycle and vertical structure of ozone in Paris, France using four years of ground based LIDAR measurements in the lowermost troposphere, Atmos. Environ., 167, 603–615, https://doi.org/10.1016/j.atmosenv.2017.08.016, 2017.

Koukouli, M.-E., Skoulidou, I., Karavias, A., Parcharidis, I., Balis, D., Manders, A., Segers, A., Eskes, H., and van Geffen, J.: Sudden changes in nitrogen dioxide emissions over Greece due to lockdown after the outbreak of COVID-19, Atmos. Chem. Phys., 21, 1759–1774, https://doi.org/10.5194/acp-21-1759-2021, 2021.

Krecl, P., Targino, A. C., Yoshikazu Oukawa, G., and Pacheco Cassino Junior, R.: Drop in urban air pollution from COVID-19 pandemic: Policy implications for the megacity of São Paulo, Environ. Pollut., 265, 114883, https://doi.org/10.1016/j.envpol.2020.114883, 2020.

Liu, F., Page, A., Strode, S. A., Yoshida, Y., Choi, S., Zheng, B., Lamsal, L. N., Li, C., Krotko, N. A., Eskes, H., van der A, R., Veefkind, P., Levelt, P. F., Hauser, O. P., and Joiner, J.: Abrupt decline in tropospheric nitrogen dioxide over China after the outbreak of COVID-19, Science Advances, 6, eabc2992, https://doi.org/10.1126/sciadv.abc2992, 2020.

Menut, L., Bessagnet, B., Siour, G., Mailler, S., Pennel, R., and Cholakian, A.: Impact of lockdown measures to combat Covid-19 on air quality over western Europe, Sci. Total Environ., 741, 140426, https://doi.org/10.1016/j.scitotenv.2020.140426, 2020.

Molina, M. O., Gutiérrez, C., and Sánchez, E.: Comparison of ERA5 surface wind speed climatologies over Europe with observations from the HadISD dataset, Int. J. Climatol., 41, 4864–4878, https://doi.org/10.1002/joc.7103, 2021.

Petit, J.-E., Dupont, J.-C., Favez, O., Gros, V., Zhang, Y., Sciare, J., Simon, L., Truong, F., Bonnaire, N., Amodeo, T., Vautard, R., and Haeffelin, M.: Response of atmospheric composition to COVID-19 lockdown measures during spring in the Paris region (France), Atmos. Chem. Phys., 21, 17167–17183, https://doi.org/10.5194/acp-21-17167-2021, 2021.

Platt, U. and Stutz, J.: Differential absorption spectroscopy, in: Differential Optical Absorption Spectroscopy, Springer Verlag, Berlin Heidelberg, https://doi.org/10.1007/978-3-540-75776-4, 2008.

Pommereau, J. P. and Goutail, F.: Stratospheric O_3 and NO_2 observations at the Southern Polar Circle in Summer and Fall 1988, Geophys. Res. Lett., 15, 895–897, 1988.

Prunet, P., Lezeaux, O., Camy-Peyret, C., and Thevenon, H.: Analysis of the NO_2 tropospheric product from S5P TROPOMI for monitoring pollution at city scale, City and Environment Interactions, 8, 100051, https://doi.org/10.1016/j.cacint.2020.100051, 2020.

Shi, X. and Brasseur, G. P.: The response in air quality to the reduction of Chinese economic activities during the COVID-19 outbreak. Geophys. Res. Lett., 47, e2020GL088070, https://doi.org/10.1029/2020GL088070, 2020.

Siddiqui, A., Halder, S., Chauhan, P., and Kumar, R.: COVID-19 Pandemic and City-Level Nitrogen Dioxide (NO_2) Reduction for Urban Centres of India, J. Indian Soc. Remot., 48, 999–1006, https://doi.org/10.1007/s12524-020-01130-7, 2020.

SAOZ: SAOZ [data set], available at: http://saoz.obs.uvsq.fr/, last access: January 2021.

Tack, F., Hendrick, F., Goutail, F., Fayt, C., Merlaud, A., Pinardi, G., Hermans, C., Pommereau, J.-P., and Van Roozendael, M.: Tropospheric nitrogen dioxide column retrieval from ground-based zenith-sky DOAS observations, Atmos. Meas. Tech., 8, 2417–2435, https://doi.org/10.5194/amt-8-2417-2015, 2015.

van Geffen, J., Boersma, K. F., Eskes, H., Sneep, M., ter Linden, M., Zara, M., and Veefkind, J. P.: S5P TROPOMI NO_2 slant column retrieval: method, stability, uncertainties and comparisons with OMI, Atmos. Meas. Tech., 13, 1315–1335, https://doi.org/10.5194/amt-13-1315-2020, 2020.

Veefkind, J. P., Aben, I., McMullan, K., Förster, H., de Vries, J., Otter, G., Claas, J., Eskes, H. J., de Haan, J. F., Kleipool, Q., van Weele, M., Hasekamp, O., Hoogeveen, R., Landgraf, J., Snel, R., Tol, P., Ingmann, P., Voors, R., Kruizinga, B., Vink, R., Visser, H., and Levelt, P. F.: TROPOMI on the ESA Sentinel-5 Precursor: A GMES mission for global observations of the atmospheric composition for climate, air quality and ozone layer applications, Remote Sens. Environ. 120, 70–83, https://doi.org/10.1016/j.rse.2011.09.027, 2012.

Verhoelst, T., Compernolle, S., Pinardi, G., Lambert, J.-C., Eskes, H. J., Eichmann, K.-U., Fjæraa, A. M., Granville, J., Niemeijer, S., Cede, A., Tiefengraber, M., Hendrick, F., Pazmiño, A., Bais, A., Bazureau, A., Boersma, K. F., Bognar, K., Dehn, A., Donner, S., Elokhov, A., Gebetsberger, M., Goutail, F., Grutter de la Mora, M., Gruzdev, A., Gratsea, M., Hansen, G. H., Irie, H., Jepsen, N., Kanaya, Y., Karagkiozidis, D., Kivi, R., Kreher, K., Levelt, P. F., Liu, C., Müller, M., Navarro Comas, M., Piters, A. J. M., Pommereau, J.-P., Portafaix, T., Prados-Roman, C., Puentedura, O., Querel, R., Remmers, J., Richter, A., Rimmer, J., Rivera Cárdenas, C., Saavedra de Miguel, L., Sinyakov, V. P., Stremme, W., Strong, K., Van Roozendael, M., Veefkind, J. P., Wagner, T., Wittrock, F., Yela González, M., and Zehner, C.: Ground-based validation of the Copernicus Sentinel-5P TROPOMI NO_2 measurements with the NDACC ZSL-DOAS, MAX-DOAS and Pandonia global networks, Atmos. Meas. Tech., 14, 481–510, https://doi.org/10.5194/amt-14-481-2021, 2021.

Viatte, C., Petit, J.-E., Yamanouchi, S., Van Damme, M., Doucerain, C., Germain-Piaulenne, E., Gros, V., Favez, O., Clarisse, L., Coheur, P.-F., Strong, K., and Clerbaux, C.: Ammonia and PM2.5 Air Pollution in Paris during the 2020 COVID Lockdown, Atmosphere, 12, 160, 1–18, https://doi.org/10.3390/atmos12020160, 2021.

WHO (World Health Organisation Europe): Air quality guidelines: Global update 2005 – particulate matter, ozone, nitrogen dioxide and sulfur dioxide, WHO Regional Office for Europe, Copenhagen, available at: https://www.euro.who.int/__data/assets/pdf_file/0005/78638/E90038.pdf (last access: 15 November 2020), 2006.

Zhou, Y., Brunner, D., Hueglin, C., Henne, S., and Staehelin, J.: Changes in OMI tropospheric NO_2 columns over Europe from 2004 to 2009 and the influence of meteorological variability, Atmos. Environ., 46, 482–495, https://doi.org/10.1016/j.atmosenv.2011.09.024, 2012.